Bull. Mater. Sci., Vol. 38, No. 7, December 2015, pp. 1723–1729. © Indian Academy of Sciences.

Facet-dependent study of efficient growth of graphene on copper by ethanol-CVD

ANIL KUMAR SINGH* and ANJAN KUMAR GUPTA
Department of Physics, Indian Institute of Technology Kanpur, Kanpur 208 016, India

MS received 10 April 2015; accepted 13 July 2015

Abstract. **The growth of graphene by chemical vapour deposition (CVD) on copper is the most promising scalable method for high-quality graphene. The use of ethanol, an economic and safe precursor, for the fast growth of graphene on copper by a home-built CVD set-up was analysed. Full coverage of uniform single-layer graphene with high crystalline quality was found on ⟨100⟩ textured Cu foils in just 30 s. The nucleation density of graphene islands was found to be independent of facets but the island shape showed facet dependence. Diamond-like islands were observed on Cu(100) facets while random shaped islands were seen on other facets. The last observation is discussed in terms of a competition between graphene-island growth and its relaxation rate on different facets. On Cu(100) slower island growth as compared to its relaxation leads to equilibrium shapes as opposed to other facets. Further, an observed evolution in graphene contrast in electron micrographs with time on different facets was discussed in terms of oxygen diffusion between graphene and Cu.**

Keywords. **Graphene; chemical vapour deposition; electron-backscattered diffraction; ethanol precursor.**

1. Introduction

Chemical vapour deposition (CVD) graphene growth on Cu has been attempted with different carbon forms, i.e., gas, liquid and solid. Methane[1,2] and ethylene[3] are the most common precursors for graphene growth. Liquids, such as hexane and alcohols,[4,5] and solids, like sugar and camphor[6,7] are preferred precursor choices owing to explosive nature of the gaseous precursors. Among liquid precursors ethanol is a safer option due to its low volatility and easy handling. Using ethanol precursor, several research groups have reported non-uniform graphene with faster growth kinetics.[8–10] Faggio *et al*[10] reported the growth of highly crystalline, few-layer graphene by CVD with ethanol using long growth time and attributed the crystalline quality of graphene to the presence of water produced from cracking of ethanol. Zhao *et al*[8] achieved self-limiting growth on copper foil enclosures with 5 min deposition time. In recent times, Lisi *et al*[9] reported full coverage of graphene on plain copper using fast growth process.

On copper, graphene growth is ascribed to surface adsorption processes,[11] leading to a uniform graphene growth. In case of low pressure (LP) CVD, graphene growth and subsequent morphology are expected to be determined by adsorption and diffusion of carbon species[12] on Cu surface and their attachment to various edges of an existing graphene island. Li *et al* studied effects of growth parameters, such as temperature, methane flow rate and partial pressure, and concluded that domain-size of graphene is determined by the initial nucleation density.[13] Vlassiouk *et al*[14] reported facet-dependent nucleation density of graphene below 1000°C, with a higher nucleation density on Cu(111) than on Cu(100) and Cu(101). However no effect of facets was seen above 1000°C. Low-index Cu facets like Cu(111) and Cu(100) have been reported to be more promising for monolayer graphene with fewer defects.[15] The growth rate on different Cu facets is reported to be different with graphene growing faster on Cu(111) than on Cu(100).[16] Different shapes,[8,17,18] such as tetragonal, four lobed, six lobed, dendritic and random, of graphene islands have been observed on Cu for graphene grown by LP-CVD. It means facets orientation of copper substrate plays an important role in graphene growth and determines the nucleation density and the island shape, which ultimately determines the quality and uniformity of graphene.[8,12,19,20]

In this paper, we study the effect of facets on nucleation density and shape of graphene islands in our LP-CVD set-up with ethanol precursor. Needle valves were used for gas flow control and to obtain uniform single layer graphene with 30 s growth time. Graphene film transferred on Si/SiO_2 substrate was characterized using Raman spectroscopy. Electron-backscattered diffraction (EBSD) images and electron micrographs show diamond-like island shapes on Cu(100) and random shapes on other facets. This is discussed in terms of competition between graphene-island growth rate and its relaxation rate on different facets. An observed evolution in graphene contrast on different facets is understood in terms of slow oxygen diffusion between graphene and Cu.

*Author for correspondence (skanil@iitk.ac.in)

2. Material and methods

2.1 *CVD set-up*

As-received Cu foil, from Alfa Aeser (#13382) with 99.8% purity, was cut into 2 × 1 cm^2 size pieces and immersed in acetic acid, acetone and 2-propanol sequentially, for 5 min in each liquid. This Cu foil is first put in 8-cm-long quartz boat, which then is placed inside a long quartz tube of one inch inner diameter in a tubular furnace. The distance between Cu substrate to carbon inlet inside the tube was kept as 20 cm. As shown in the schematic in figure 1, two needle valves (NV-1 and NV-2), two shut off valves (SV-1 and SV-2) and a multi-turn valve (MTV) were used in the experimental set-up. The pressure inside the quartz tube is controlled by NV-2 and MTV. The pressure regulated Ar/H_2 (5% H_2 in Argon) gas-line bifurcates into two paths, A and B. The path-A allows the gas flow directly through the long quartz tube while the path-B allows the gas flow via the sealed ethanol flask. The path-A is used during heating, annealing and cooling while the path-B is used for graphene growth. Initially the gas mixture was flowed via the path-B while pumping via MTV and NV-2 in order to flush out any atmospheric gas from the flask and between SV-2 and NV-2.

After inserting the quartz boat with Cu foil, the furnace temperature is set to 980°C. SV-1 was opened to flow the gas through the path-A while pumping through MTV. NV-1 is adjusted so as to get the pressure inside quartz tube around 10 mbar while keeping the outlet pressure of the regulator as 1.17 bar. The same pressure inside the quartz tube is used whenever the gas flows along the path-A, which is the case during heating, annealing and cooling. After temperature reaches 980°C we wait for 20 min in order to anneal the Cu foil in this 10 mbar Ar–H_2 mixture and to remove oxide from Cu surface. After this annealing, SV-1 was closed and the gas flow was allowed through the path-B (via ethanol container) by opening NV-2 by two turns such that the growth pressure inside the quartz tube is 0.2 mbar. The gas flow rate was separately calibrated through NV-2, when it is opened by two turns, as 30 ml h^{-1}. Depending on growth requirement NV-2 was closed after a specified time (between 10 and 30 s). After this step the gas flow was directed through the path-A. The furnace was then turned off and the quartz tube was shifted so as to bring its central portion, containing Cu foil, to outside the furnace at ambient temperature. This cools the foil quite fast. The gas flow was stopped after an hour and the tube was opened to take out the Cu foil.

2.2 *Transfer of CVD graphene*

In above CVD process, graphene grows on both sides of Cu foil, while graphene was transferred only from the top side to SiO_2/Si surface. For transfer, 950k poly-methyl methacrylate (PMMA) solution (4.0% in Anisole) was spun on top side of Cu foil at 2000 rpm, followed by a bake-out at 120°C for 5 min. After this, the foil with PMMA was floated facing up in 10% HNO_3 solution for 10 min to remove the back side graphene. Cu was then etched using 1.5 M-Fe$(NO_3)_3$ solution followed by rinsing in deionized water. This graphene supported on PMMA was then scooped out from deionized water on a SiO_2 (300 nm)/Si (0.5 mm, n-doped) substrate. After keeping it for 24 h in clean environment it was heated on a hot plate at 150°C for 15 min to get better adhesion of graphene with the substrate.[21] This substrate was then immersed in warm acetone (60°C) for 3 h to dissolve PMMA followed by rinsing in 2-propanol.

2.3 *Characterization details*

A Zeiss SEM (Model: EVO-18 with LaB_6 filament) with 5 kV beam voltage and Everhart-Thornley (ET) secondary electron detector was used to study the graphene morphology on Cu foil. A commercial ambient Raman spectroscopy

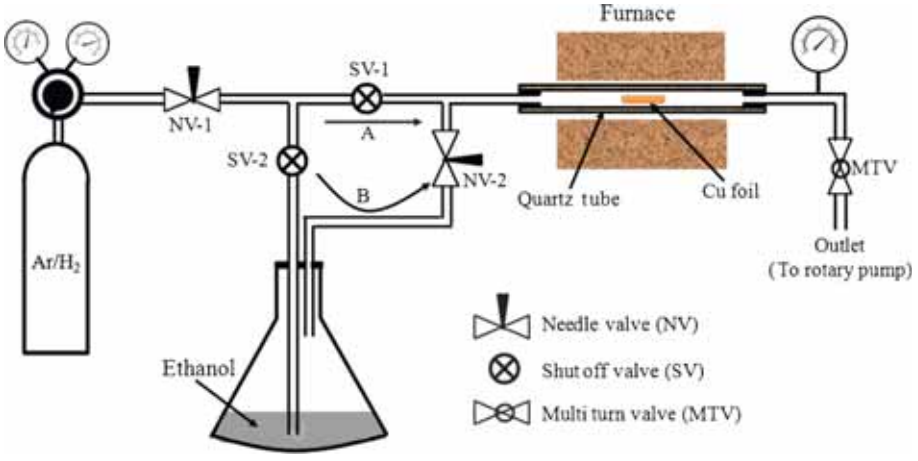

Figure 1. Schematic of home-built LP-CVD set-up. Path-A allows the gas flow directly through the sample-tube while path-B allows the gas flow through sample-tube via the sealed ethanol flask. For graphene growth, Ar/H_2 follows path-B (see text for details).

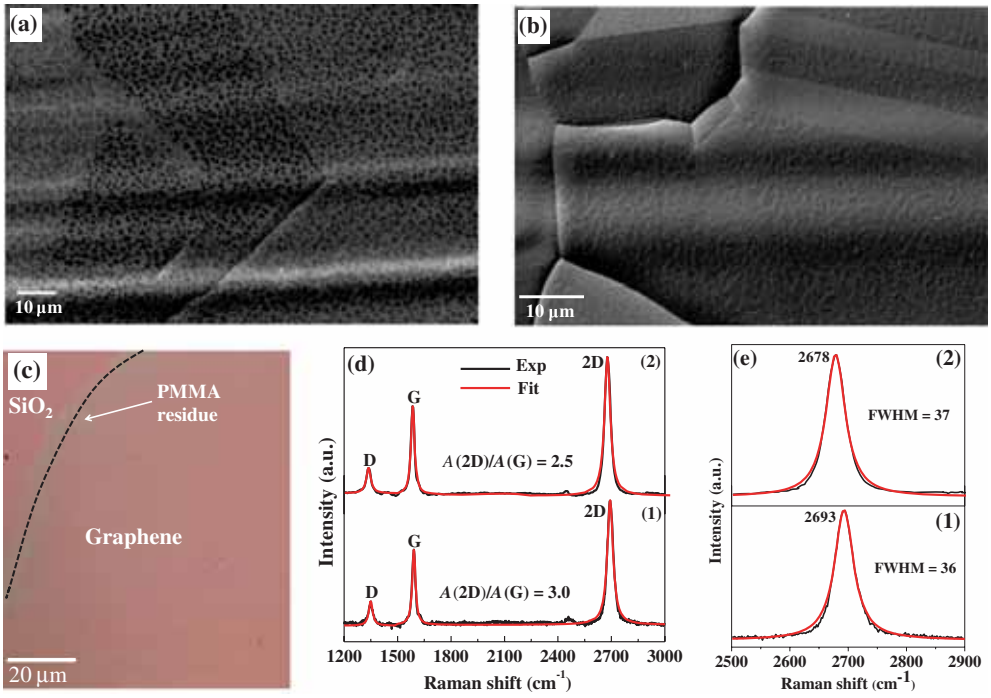

Figure 2. SEM images of as-grown graphene on Cu surface with fixed growth pressure with different growth times **(a)** 10 s, **(b)** 30 s. **(c)** Optical micrograph of a graphene film on a SiO_2/Si substrate; dotted line shows interface between graphene and SiO_2. **(d)** The Raman spectra at two different points of graphene on SiO_2/Si substrate and their Lorentzian fit. **(e)** Enlarged view of the 2D band with their Lorentzian fits.

set-up (spot size 0.5 μm, wavelength 532 nm) was used to determine the quality and number of layers in deposited graphene on SiO_2/Si substrate. X-ray diffraction (XRD) using CuK_α radiation ($\lambda = 1.54$ Å) with scan rate 0.5 deg min^{-1} and EBSD orientation mapping using a different SEM (Zeiss SEM, EVO-50) were used to determine the facets present in the Cu foil.

3. Results and discussions

3.1 *Synthesis and characterization of graphene*

The graphene coverage on copper as a function of growth time was studied while keeping other parameters, i.e., temperature (980°C), pressure (0.2 mbar), etc., fixed. Figure 2a shows the SEM images of as-grown graphene on Cu surface for 10 s deposition time showing higher nucleation density as compared to the ones reported with methane precursor. Graphene islands' size and separation between islands are of 1 μm order. With 30 s growth time, full coverage of graphene on copper surface was achieved as shown in figure 2b. Graphene domain size increases with growth time without significant change in nucleation density. In 30 s the domain size increases to around 3 μm. Figure 2c shows the white light optical micrograph of transferred graphene on 300 nm SiO_2/Si substrate. The transfer process leaves behind some PMMA residue on graphene. Figure 2d shows the Raman spectra of transferred graphene, with Lorentzian fits, at two random places [marked as (1) and (2)]. It shows characteristic Raman features, namely the D-band, G-band and 2D band, of graphene. The presence of Raman D-peak indicates that the transferred graphene has defects. Enlarged view of the 2D peak of both spectra with their Lorentzian fits is shown in figure 2e. Table 1 shows various parameters found from the two representative Raman spectra. Here, the frequency integrated intensity ratios have been found from the ratios of the areas under the respective Raman peaks. The small FWHM value,[22] high (more than 2.0) $A(2D)/A(G)$[23] value and the single Lorentzian fitting of the 2D peak[24] have been used in literature as characteristics of monolayer graphene. AFM imaging on this 30 s CVD graphene sample on SiO_2 shows graphene height to be in 2–3 nm range. This was found to be same as that of mechanically exfoliated monolayer (confirmed by Raman) graphene. The reported values of the monolayer graphene (CVD) height, as found from AFM, on SiO_2 are above 1 nm.[4,25,26] This is significantly more than the interlayer separation, i.e., 0.34 nm, in graphite.

3.2 *Graphene nucleation density and morphology*

The crystallographic orientation of the Cu foil affects carbon adsorption,[27] surface diffusion[28] and dehydrogenation[29] leading to different growth on different facets. In order to investigate the role of Cu facets on graphene morphology, XRD and EBSD mapping of the Cu foil was performed.

Table 1. Summary of two representative Raman spectra using Lorentzian peak fits.

Spectra	D peak	G peak	2D peak	A(2D)/A(G)	A(D)/A(G)
1				3.0	0.39
Peak position (cm^{-1})	1349	1591	2693		
FWHM (cm^{-1})	26	22	36		
2				2.5	0.36
Peak position (cm^{-1})	1337	1585	2678		
FWHM (cm^{-1})	31	25	37		

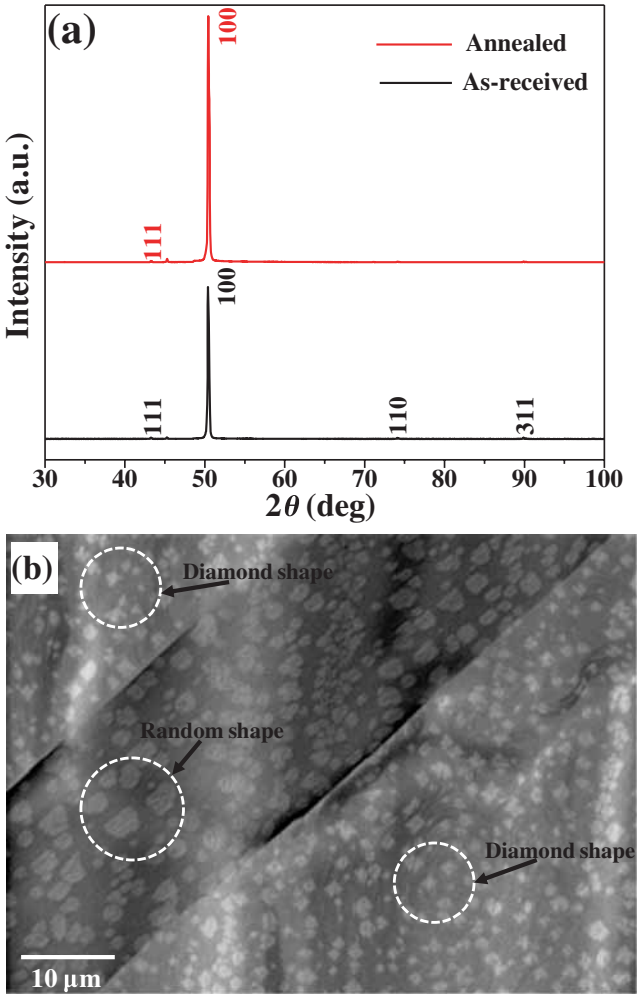

Figure 3. **(a)** XRD of Cu foil as-received and annealed state (CVD process was stopped just before the deposition, i.e., after 20 min Ar/H_2 annealing). **(b)** SEM image of graphene islands on different Cu facets after 10 s growth.

Figure 3a shows XRD of as-received Cu foil as well as that of Ar/H_2 annealed foil. The as-received Cu foil shows ⟨100⟩ texture with small fractions of (111), (110) and (311) grains. Post-annealed Cu has higher ⟨100⟩ texture[30] with very small fraction of (111) grains. The width of (100) peak is also reduced due to annealing indicating an increase in grain size. Figure 3b shows SEM image after 10 s CVD growth with three different Cu grains separated by two, almost straight-line, edges. There is no effect of Cu grain boundary on graphene nucleation density. As seen in figure 3b, on two of the three grains the graphene islands have diamond-like shape[31] (a quadrilateral with two pairs of equal-length sides and equal opposite-angles) while the third grain shows random shape islands.

Figure 4 shows the EBSD map, after 10 s graphene growth, together with SEM images of its selected regions. Figure 4a shows the z-direction inverse-pole map of a selected region of the Cu foil depicting various facets, such as (100), (111) and (110). From this figure it is confirmed that Cu(100) facets cover a large fraction (70–80%) of the Cu surface. We would like to point out that this Cu foil is not single crystalline as seen from both XRD plot and EBSD image. Figure 4b and c shows the SEM images of regions marked as 1 and 2 in figure 4a. On further zooming into these selected areas it was clearly seen that graphene nucleation density is independent of facets. This is in contrast with the report of Vlassiouk *et al*[14] who found a facet-dependent nucleation density of graphene below 1000°C. The graphene island shape was found to be diamond-like on Cu(100) facet and rounded random shape on other facets. The diamond-like shape is consistent with the four-fold symmetry of the Cu(100) facet. On the same Cu foil (Alfa Aeser, #13382) using LP-CVD with gaseous precursors, diamond-like or four-lobed islands[2,13,32] as well as tetragonal, circular or random shaped islands[2,17,32–34] have been reported.

Both experiments[8,12,19,20,35] and simulations[12,28,35] have been tried to address the growth mechanism, shape of graphene islands on various Cu facets. During the CVD growth carbon containing species strike the copper surface homogeneously and some of these get strongly pinned to the surface due to defects acting as nucleation sites, others adsorb but they are still mobile on the Cu surface. In case of local super-saturation of carbon species the nucleation site can also be created on defect-free Cu surface.[13] The mobile carbon species (hydrocarbon) will diffuse and get attached with already nucleated sites after partial dehydrogenation. Thus the graphene islands will grow. Hence the three sub-processes involved are adsorption of carbon species on the surface, its diffusion and attachment to an existing island. In order to understand the shape of graphene islands, some groups give more importance to diffusion, which is presumed to be surface limited.[8,12,36] In this case the island shapes are facet dependent because the anisotropy in carbon-species-diffusivity is facet dependent.[37] Others have attributed the

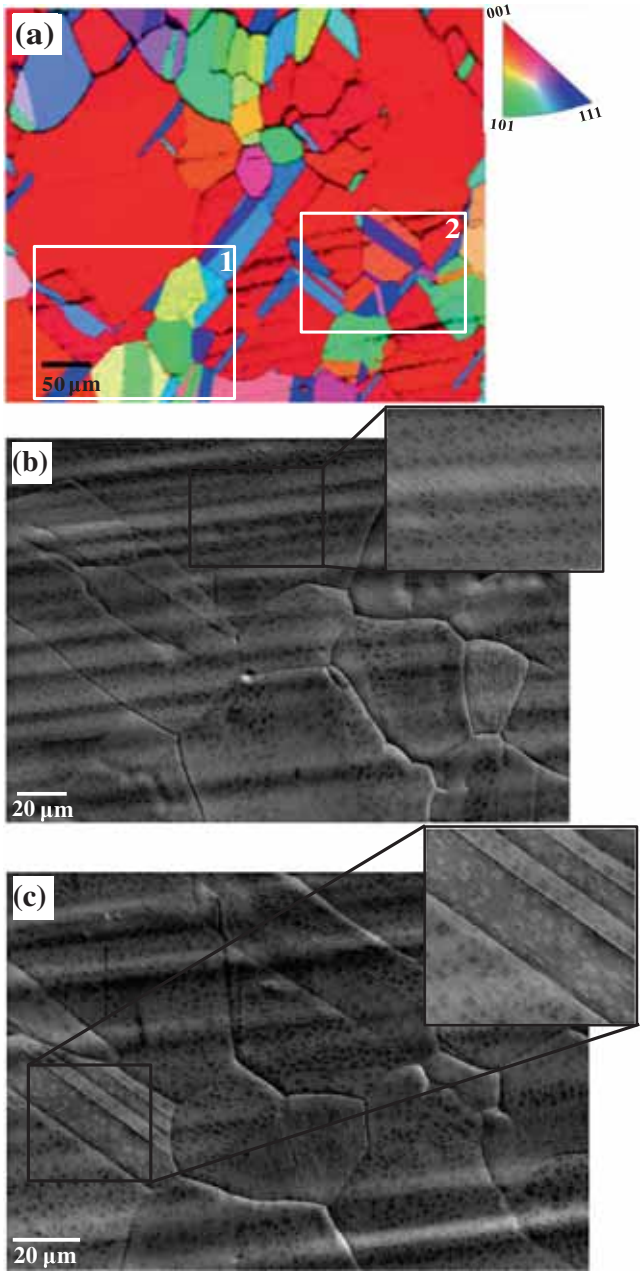

Figure 4. EBSD map and SEM images of its selected regions after 10 s graphene growth. **(a)** The *z*-direction EBSD map of a selected region of the Cu foil containing various facets, such as (100), (111), (110) and other higher index. The inset shows inverse pole colour index. **(b)** and **(c)** show the SEM images of regions marked as 1 and 2 in **a**. The inset of **b** and **c** shows further zoomed-in images to resolve graphene island shapes. It can be seen that on Cu(100) facet islands are diamond-like and on other facets they have random shapes.

facet dependent shape to the anisotropy in the attachment of carbon species at the growing front of an island.[35] In general, both diffusion and attachment anisotropies will play a role in the final island shape. Another process relevant here is the relaxation of the islands which can happen by edge diffusion of carbon species.[12] The carbon species will initially attach to a graphene island at a random site on the edge and then it will

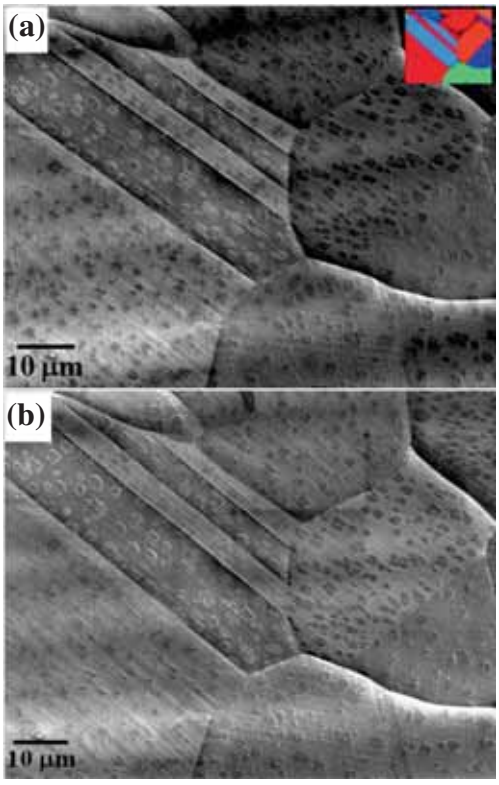

Figure 5. SEM contrast evolution: **(a)** shows the SEM image acquired 2 weeks after CVD growth. The inset shows EBSD map for SEM region. **(b)** SEM image of same region as **a** but acquired 3 weeks after CVD growth. The contrast of graphene islands on Cu(111) is changed between the two images.

try to find more energetically favourable location. In this case the island shape and symmetry will eventually be determined by the underlying facet. The interplay between island growth rate and its relaxation rate will also play an important role independent of the growth itself (determined by adsorption, diffusion and attachment) being biased towards a particular shape on a given facet. In fact the growth process itself may not necessarily give rise to the minimum energy shape. It is widely reported that slow growth rates achieved by reduction of partial pressure of carbon species, give rise to four lobed shape on Cu(100) and six lobed shape on Cu(111).[8,36] Thus if the islands are given enough time to relax during growth, the growth process may not play much role in dictating the shape. The island relaxation rate may also be facet dependent while it is reported that on Cu(111) the growth rate is higher than Cu(100).[16] The latter implies that less time is available for relaxation on Cu(111) as compared to Cu(100) giving more equilibrium shapes on later. As a result four lobed shape on Cu(100) are more often seen than six lobed shapes on Cu(111)[36] and the later requires slower and longer growth by reducing the partial pressure of carbon species.

3.3 *SEM contrast evolution*

Figure 3b shows that graphene islands appear brighter than Cu in secondary-emission (with ET detector) SEM images.

This is believed to happen due to oxidation of Cu region, uncovered by grapheme.[38] Graphene appears brighter as it blocks less number of secondary electrons[39] than copper oxide. The SEM image in figure 3b was acquired almost immediately after CVD growth; however the exposed Cu had enough time ($\sim$ 30 min) to oxidize. If the SEM images are acquired after more delay, it was found that the contrast on other than Cu(111) facets is reversed, i.e., graphene appears darker than Cu. This can be seen in SEM image in figure 5a, which was acquired 2 weeks after CVD growth. However, the contrast on other facets is preserved. With more time, even Cu(111) facets go through the same contrast reversal as seen in SEM image in figure 5b, which was taken 3 weeks after CVD growth. We store the samples in vacuum desiccators when not in use but the presence of oxygen cannot be ruled out.

It is believed that this contrast reversal occurs due to oxygen diffusion inbetween graphene islands and Cu, thus more number of secondary electrons are blocked wherever there is graphene. This makes graphene islands appear darker with time. Both contrasts have been reported in literature without much discussion on their origin. Slower contrast reversal on Cu(111) facets is presumably due to slower oxygen diffusion between graphene and Cu(111) surface as compared to other facets. This is further strengthened by the report of Shi *et al*[40] that graphene bonding on Cu(111) is stronger as compared to Cu(100) and Cu(110). This can lead to slower diffusion of oxygen between Cu and graphene on Cu(111) facets.

4. Conclusions

An ethanol-based inexpensive LP-CVD set-up for rapid and efficient graphene synthesis was described. Full coverage of uniform single layer graphene is achieved on ⟨100⟩ textured Cu foils in 30 s. By correlating electron microscopy images with the EBSD maps nucleation density of graphene islands was found to be independent of facet orientation. Diamond-like islands are seen on Cu(100) while on the other facets the islands have random shapes. This last result was attributed to slower growth, as compared to relaxation, of graphene islands on Cu(100) as compared to other facets. A time evolution of SEM contrast on different Cu facets is understood using facet-dependent diffusion of oxygen between Cu and graphene islands.

Acknowledgements

We thank Rajeev Gupta for Raman measurements and acknowledge CSIR of the Government of India for financial support.

References

1. Kim K S, Zhao Y, Jang H, Lee S Y, Kim J M, Kim K S, Ahn J H, Kim P, Choi J Y and Hong B H 2009 *Nature* **457** 706
2. Li X, Cai W, An J, Kim S, Nah J, Yang D, Piner R, Velamakanni A, Jung I, Tutuc E, Banerjee S K, Colombo L and Ruoff R S 2009 *Science* **324** 1312
3. Coraux J, N'Diaye A T, Busse C and Michely T 2008 *Nano Lett.* **8** 565
4. Srivastava A, Galande C, Ci L, Song L, Rai C, Jariwala D, Kelly K F and Ajayan P M 2010 *Chem. Mater.* **22** 3457
5. Guermoune A, Chari T, Popescu F, Sabri S S, Guillemette J, Skulason H S, Szkopek T and Siaj M 2011 *Carbon* **49** 4204
6. Sun Z, Yan Z, Yao J, Beitler E, Zhu Y and Tour J M 2010 *Nature* **468** 549
7. Sharma S, Kalita G, Hirano R, Hayashi Y and Tanemura M 2013 *Mater. Lett.* **93** 258
8. Zhao P, Kumamoto A, Kim S, Chen X, Hou B, Chiashi S, Einarsson E, Ikuhara Y and Maruyama S 2013 *J. Phys. Chem. C* **117** 10755
9. Lisi N, Buonocore F, Dikonimos T, Leoni E, Faggio G, Messina G, Morandi V, Ortolani L and Capasso A 2014 *Thin Solid Films* **571** 139
10. Faggio G, Capasso A, Messina G, Santangelo S, Dikonimos T, Gagliardi S, Giorgi R, Morandi V, Ortolani L and Lisi N 2013 *J. Phys. Chem. C* **117** 21569
11. Li X, Cai W, Colombo L and Ruoff R S 2009 *Nano Lett.* **9** 4268
12. Nie S, Wofford J M, Bartelt N C, Dubon O D and McCarty K F 2011 *Phys. Rev. B* **84** 155425
13. Li X, Magnuson C W, Venugopal A, An J, Suk J W, Han B, Borysiak M, Cai W, Velamakanni A, Zhu Y, Fu L, Vogel E M, Voelkl E, Colombo L and Ruoff R S 2010 *Nano Lett.* **10** 4328
14. Vlassiouk I, Smirnov S, Regmi M, Surwade S P, Srivastava N, Feenstra R, Eres G, Parish C, Lavrik N, Datskos P, Dai S and Fulvio P 2013 *J. Phys. Chem. C* **117** 18919
15. Zhao L, Rim K T, Zhou H, He R, Heinz T F, Pinczuk A, Flynn G W and Pasupathy A N 2011 *Solid State Commun.* **151** 509
16. Wood J D, Schmucker S W, Lyons A S, Pop E and Lyding J W 2011 *Nano Lett.* **11** 4547
17. Liu W, Li H, Xu C, Khatami Y and Banerjee K 2011 *Carbon* **49** 4122
18. Zhang Y, Zhang L, Kim P, Ge M, Li Z and Zhou C 2012 *Nano Lett.* **12** 2810
19. Rasool H I, Song E B, Mecklenburg M, Regan B C, Wang K L, Weiller B H and Gimzewsk J K 2011 *J. Am. Chem. Soc.* **133** 12536
20. Wofford J M, Nie S, McCarty K F, Bartelt N C and Dubon O D 2010 *Nano Lett.* **10** 4890
21. Liang X, Sperling B A, Calizo I, Cheng G, Hacker C A, Zhang Q, Obeng Y, Yan K, Peng H, Li Q, Zhu X, Yuan H, Walker A R H, Liu Z, Peng L and Richter C A 2011 *ACS Nano* **5** 9144
22. Lee D S, Riedl C, Krauss B, Klitzing K V, Starke U and Smet J H 2008 *Nano Lett.* **8** 4320
23. Okano M, Matsunaga R, Matsuda K, Masubuchi S, Machida T and Kanemitsu Y 2011 *Appl. Phys. Lett.* **99** 151916
24. Ferrari A C, Meyer J C, Scardaci V, Casiraghi C, Lazzeri M, Mauri F, Piscanec S, Jiang D, Novoselov K S, Roth S and Geim A K 2006 *Phys. Rev. Lett.* **97** 187401
25. Lenski D R and Fuhrer M S 2011 *J. Appl. Phys.* **110** 013720
26. Chung T F, Shen T, Cao H, Jauregui L A, Wu W, Yu Q, Newell D and Chen Y P 2013 *Int. J. Mod. Phys. B* **27** 1341002

27. Pang X Y, Xue L Q and Wang G C 2007 *Langmuir* **23** 4910
28. Fan L, Zou J, Li Z, Li X, Wang K, Wei J, Zhong M, Wu D, Xu Z and Zhu H 2012 *Nanotechnology* **23** 115605
29. Zhang W, Wu P, Li Z and Yang J 2011 *J. Phys. Chem. C* **115** 17782
30. Vlassiouk I, Fulvio P, Meyer H, Lavrik N, Dai S, Datskos P and Smirnov S 2013 *Carbon* **54** 58
31. Wu C, Li F, Chen W, Veeramalai C P, Ooi P C and Guo T 2015 *Sci. Rep.* **5** 9034
32. Jia C, Jiang J, Gan L and Gu X 2012 *Sci. Rep.* **2** 707
33. Celebi K, Cole M T, Teo K B K and Park H G 2012 *Electrochem. Solid-State Lett.* **15** K1
34. Yang F, Liu Y, Wu W, Chen W, Gao L and Sun J 2012 *Nanotechnology* **23** 475705
35. Kim H, Mattevi C, Calvo M R, Oberg J C, Artiglia L, Agnoli S, Hirjibehedin C F, Chhowalla M and Saiz E 2012 *Am. Chem. Soc. Nano* **6** 3614
36. Jacobberger R M and Arnold M S 2013 *Chem. Mater.* **25** 871
37. Hu T, Zhang Q, Wells J C, Gong X and Zhang Z 2010 *Phys. Lett. A* **374** 4563
38. Celebi K, Cole M T, Choi J W, Wyczisk F, Legagneux P, Rupesinghe N, Robertson J, Teo K B K and Park H G 2013 *Nano Lett.* **13** 967
39. Xie J and Spallas J P 2012 *Agilent Technologies* (URL-http://www.toyo.co.jp/file/pdf/spm/files/agi/5991-0782EN.pdf, 8 April 2015)
40. Shi X, Yin Q and Wei Y 2012 *Carbon* **50** 3055